

Doppler estimation and correction for shallow underwater acoustic communications

Kenneth A. Perrine*, Karl F. Nieman*, Terry L. Henderson*, Keith H. Lent*, Terry J. Brudner* and Brian L. Evans†

*Applied Research Laboratories

†Dept. of Electrical and Computer Engineering,

The University of Texas at Austin, Austin, TX 78712

{kperrine, knieman}@mail.utexas.edu, {lent, henderson, brudner}@arlut.utexas.edu, bevans@ece.utexas.edu

Abstract—Reliable mobile underwater acoustic communication systems must compensate for strong, time-varying Doppler effects. Many Doppler correction techniques rely on a single bulk correction to compensate first-order effects. In many cases, residual higher-order effects must be tracked and corrected using other methods. The contributions of this paper are evaluations of (1) signal-to-noise ratio (SNR) performance from three Doppler estimation and correction methods and (2) communication performance of Doppler correction with static vs. adaptive equalizers. The evaluations use our publicly available shallow water experimental dataset, which consists of 360 packet transmission samples (each 0.5s long) from a five-channel receiver array.

I. INTRODUCTION

Wireless signals experience a variety of degradations due to channel imperfections [1], [2]. Just as electromagnetic signals are subject to a number of channel effects, including attenuation, reflections, and interference, underwater acoustic signals are subject to the same effects. One key difference between the RF and underwater acoustic channels is propagation speed. The $\sim 200,000$ times slower sound speed in water makes time-varying Doppler effects much more pronounced [3].

When compared to many RF wireless communication signals, underwater communication signals are wideband, often operating at very low Q-factors [4], [5]. It therefore cannot be assumed that Doppler effects are treatable with a uniform frequency shift. Also, a highly reflective, changing surface and strong, refractive gradients further complicate the channel [6].

At The University of Texas Applied Research Laboratory (ARL), we have been investigating methods of sending data acoustically through water. In Nov. 2009 at ARL's Lake Travis Test Station (Fig. 1), we observed that transmitted communication signals were drastically affected by the lake environment [7]. Analysis of the data revealed two prohibitive impairments common to the shallow underwater acoustic channel (SUWA): (1) high energy, long time constant reverberation and (2) significant, time-varying Doppler effects with time constants on the order of our packet lengths. Fig. 2 shows how Doppler effects can affect a received signal. Several authors have reported similar challenges in underwater tests [2], [8].

In this paper, we report our process in decoding signals transmitted over a distance of 30 to 1285 m in a shallow underwater (SUWA) channel approx. 37 m deep. We compare

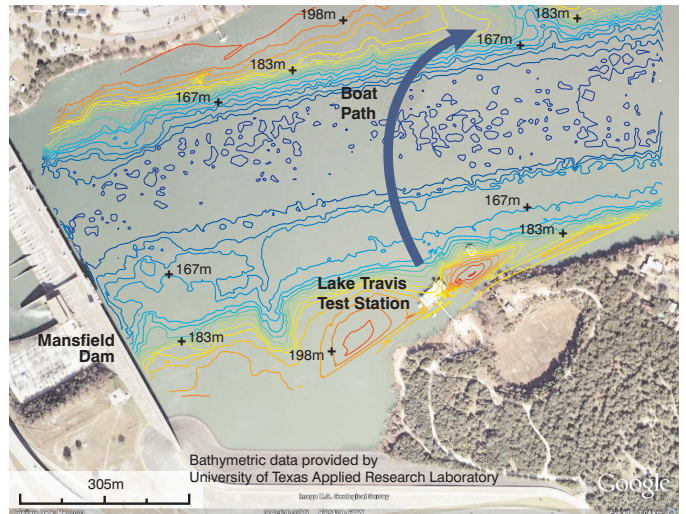


Fig. 1. Aerial view of the Lake Travis test environment with lake bed elevations given above sea level. The water level is 198 m. The five receivers are located at the Lake Travis Test Station. Figure reprinted from [7].

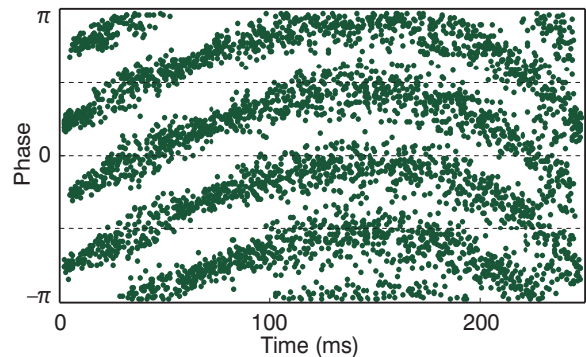


Fig. 2. Typical residual Doppler effects on the phase of a received QPSK signal after a bulk Doppler offset correction. Voronoi regions for the maximum-likelihood detector are denoted by dashed lines. Here, maximum phase error is apparent at the peak offset near 150ms.

the SNRs after applying three Doppler compensation techniques, and then analyze static and adaptive equalization. We also introduce the dataset, available at <http://users.ece.utexas.edu/~bevans/projects/underwater/datasets/>.

II. BACKGROUND

An important first step in Doppler compensation is to estimate the average bulk Doppler shift. This can be done by simply measuring the frequency offset of a pilot tone. Another class of techniques uses matched filtering to measure the time distance between two or more known transmissions. Any deviation from the expected time difference can be interpreted as a time dilation that is proportional to Doppler shift. Such transmissions can be repetitions of a waveform having high time-bandwidth product such as pseudo-noise sequences or linear frequency modulation (LFM) chirps [9]. LFM chirps are a good choice because of their resilience against severe Doppler effects. A variant of this idea, proposed by Moose, allows frequency offset to be estimated from the phase of the cross-correlation between two successively repeated, basebanded symbol sequences [10]. These repeated sequences are considered as *self-referencing*. Alternatively, the single Doppler shift can be determined by measuring the dominant frequency offset in a discrete Fourier transform (DFT) of a power-law rectified PSK sequence. For a BPSK signal, rectification is achieved by squaring the received samples; for QPSK, the samples must be raised to the power of 4. An important caveat is that noise power is also increased by rectification.

We improve upon an overall packet-wide correction by responding to time-varying residual Doppler effects through piecewise estimation and correction. For example, PSK-modulated packets can be partitioned into windows and individually analyzed by rectifying, performing a DFT, and observing the dominant frequency offsets. Alternatively, the phased lock loop (PLL) is a common technique for discovering time-varying offsets in frequency [11], [12]. PLLs can track phase changes in PSK-modulated waveforms as well as pilot tones situated outside of the data signal band, but can be challenging to properly configure in quickly varying channels with multipath.

Other techniques for Doppler detection exist. One paper reports the use of cross-correlation over one sequence of training data at the start of each packet to estimate frequency offset, followed by the use of a phase-locked loop that is closely coupled with its decision feedback equalizer [13]. Another paper ambitiously addresses open-sea OFDM underwater communications by using cross-correlation to find preamble and postamble sequences on each packet to estimate the overall frequency offset, analyzing unwanted energy in a set of null subcarriers that may be present because of residual Doppler effects, and then tracking phase offsets in pilot tones [14].

For our work, we estimated Doppler shift using three different methods. The first estimated the average bulk Doppler shift using self-referenced correlation. The second tracked time-varying Doppler effects through windowed DFT. The third measured pilot tone frequency over intervals of time.

III. METHODOLOGY

A. Waveform Design

We designed the waveform to satisfy four objectives. First, the transmitter and receiver frequency response prompted the

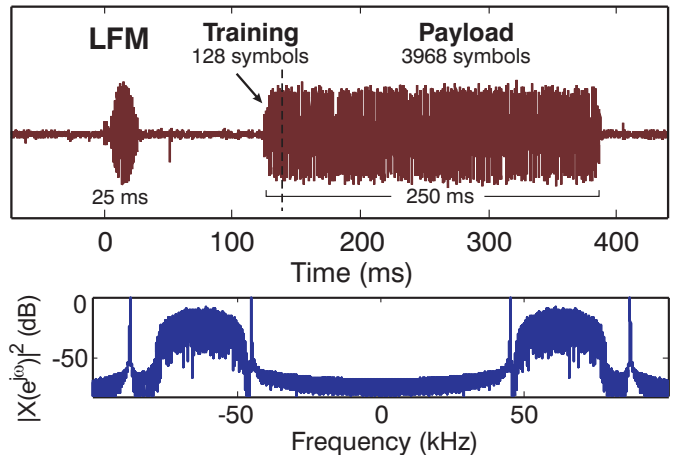


Fig. 3. Packet structure used for the test and its transmitted spectrum, showing the 45kHz and 87kHz pilot tones. The waveform pictured is sampled from a 230 m long shallow underwater channel.

use of a 62.5 kHz center frequency with a bandwidth of 31.25 kHz. Second, the waveform was structured to resemble a practical design that is suitable for data communication applications. We employed QPSK modulation, using a square root raised cosine pulse shape with a rolloff factor of 1. The packet consisted of 4096 symbols at a symbol rate of 15.625 kHz. Third, we also incorporated elements that facilitate analysis of reverberation in the channel. The waveform contained 100 ms gaps of silence to reduce inter-packet interference in this experiment, and a single data packet was preceded with an LFM chirp for the purpose of measuring the channel impulse response over 100 ms. The LFM chirp also facilitated the automatic time registration of packets after initial sampling. Finally, the design incorporated features that are specific to the frequency offset and Doppler detection techniques that we are analyzing. Specifically, two pure pilot tones were added at 45 kHz and 87 kHz to facilitate phase tracking, and four repetitions of a length 13 Barker sequence were added to allow for self-referencing frame synchronization and frequency offset detection [9]. Furthermore, 76 symbols followed the Barker sequences and were used for equalizer training. Fig. 3 shows the packet structure and the transmitted waveform spectrum.

To better understand the SUWA channel, we plot channel impulse responses for near and far ranges in Fig. 4. Longer reverberation time constants and more complex power delay profiles are often observed as range increases. The loudest path is not always the earliest received path, especially for far range. Attenuation also varies with frequency and transmit power [15].

B. Data Collection

Data was collected Nov. 6, 2009 at the ARL Lake Travis Test Station. The lake, with an estimated depth of 37 m [16], offers a number of challenges in data communication, including seasonal thermoclines that cause changes in the directional

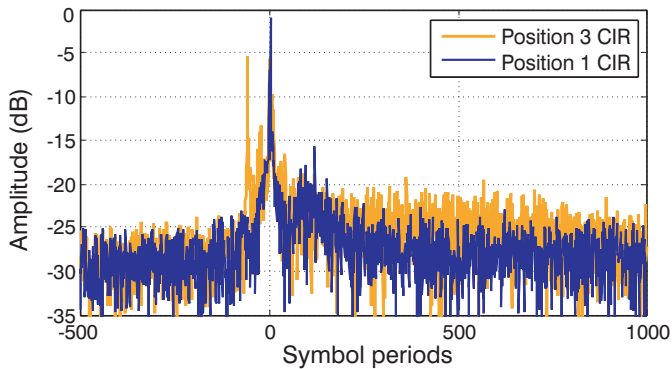


Fig. 4. Channel impulse responses (CIR) for near and far ranges. Position 1 range is 30 m and Position 3 range is ~ 1260 m.

tendency of sound propagation, reflections from the flat concrete surface of Mansfield Dam, and line-of-sight blockage from the hilly terrain of the former riverbed (see Fig. 1).

The omnidirectional transducer used to transmit the waveforms was connected to an amplified DAC operating at a 500 kHz sample rate. At unity gain, the transducer placed about 1 W of acoustic power into the water. It was tethered to a boat at various depths between 1 m and 8 m. The receiver consisted of a flat, planar array of 5 directional hydrophones with horizontal and vertical half-power beamwidths of approx. 45° and 10° , respectively. The array was submerged to a depth of 4.6 m at the test station. Hydrophone signals were preamplified and sampled at 200 kHz by a 1 MHz multiplexed DAC.

The positions used for analysis are shown in Table I. Pos. 2 through Pos. 4 distances reported in the table vary by about 50 m due to boat drift experienced during each data collection cycle. While Pos. 1 through Pos. 3 involve the stationary placement of the transducer at depths of 2.1 m and 8.3 m, Pos. 4 features a vertical, oscillating motion of about 0.5 Hz (from about 5.7 m to 7.2 m) to simulate boat motion from heavy waves, and Pos. 5 involves the towing of the transducer at speeds of ~ 5 km/h at varying depths no greater than 5 m. In total, 360 data packets were recorded over a 2-hour span. A representative subset of 29 packets was used in this preliminary analysis.

TABLE I
BOAT AND TRANSDUCER POSITIONS.

Pos.	Range	Motion	TX Gain
1	15 m	Docked to barge	-13 dB
2	325 - 375 m	Free-floating	-7 dB
3	1235 - 1285 m	Free-floating	-3 dB
4	185 - 255 m	Simulated vertical "wave" motion	-7 dB
5	300 - 80 m	Towing at ~ 3 kts	-10 dB

C. Software Receiver

The software receiver consists of a frame synchronizer, a Doppler detection stage, a Doppler compensator (via resampling), and an equalizer stage. These stages initially take one packet of received samples as input and then execute a given selection of Doppler detection and equalizer implementations.

First, the frame synchronizer identifies the presence of an LFM chirp which precedes the data frame. At this stage the received signal is basebanded and decimated to 4x the symbol rate. Finer frame synchronization is then achieved through a self-referenced Barker sequence correlation.

Second, one of three Doppler detection algorithms is performed. The first determines the overall time dilation that is proportional to the Doppler shift over the set of Barker sequences [10]. The second involves the use of windowed DFT to measure the frequency offset of the rectified sequence within each window. We select among 1 (the entire 250 ms data sequence), 2 (each 125 ms), 4 (each 62.5 ms), and 8 (each 31.25 ms). The third measures pilot tone frequency, and uses the same window configurations. Although our packets contain two pilot tones, we had found that the upper tone (87 kHz) was better positioned within the receiver's operational frequency range and therefore had a stronger signal. The pilot tone is filtered by an ideal 1.25 kHz bandpass filter to accommodate up to a $\pm 1\%$ frequency shift before it is analyzed.

Third, Doppler correction is applied using the results from the second stage. We upsample the 4x oversampled basebanded sequence by a factor of 10, linearly interpolate to restore symbol timing, and multiply by a phase correction factor to restore the phase information of the carrier. The linear interpolations are performed according to a series of D piecewise cubic splines derived from the Doppler detector's frequency offsets, where D is the number of windows.

The final stage employs a fractionally spaced decision feedback equalizer (DFE) structure that operates on the 4x oversampled sequence [17]. The equalizer uses 5 fractionally spaced (4x symbol rate) forward and 3 decision feedback taps. Equalizer coefficients are initialized to the least squares solution over the training sequence. The payload data is then processed by (1) the static DFE or (2) a decision-directed adaptive DFE with a learning rate of 0.01.

D. Analysis Framework

In our experiment, the analysis framework processes the received waveform with the software receiver using one of 9 different Doppler estimation configurations (as listed in Table II). We measure the uncoded bit error rate (BER), and estimate the SNR at the equalizer output according to:

$$SNR_{est} = 20 \log_{10} \left(\frac{R_s}{R_e} \right) \quad (1)$$

Here, R_s is the RMS signal magnitude that coincides with the expected symbol position within the QPSK constellation, and R_e is the RMS error vector magnitude, which is the distance of the sampled symbol from the expected constellation position.

While this SNR estimate is useful for comparing relative performance, the accuracy of this estimate degrades when true SNR gets low (< 5 dB), as MMSE equalizers tend to shrink tap coefficients and center received symbols in the constellation when subject to high noise. The BER measurement is instrumental in quickly determining the receiver's success in decoding the data. Small BER rates can be tolerated in systems that employ error correcting codes [17], [18].

TABLE II
DOPPLER ESTIMATION CONFIGURATIONS.

	A	B	C	D	E
Method	Moose	DFT	DFT	DFT	DFT
# Windows $D =$	1	1	2	4	8
	F	G	H	I	
Method	Pilot	Pilot	Pilot	Pilot	
# Windows $D =$	1	2	4	8	

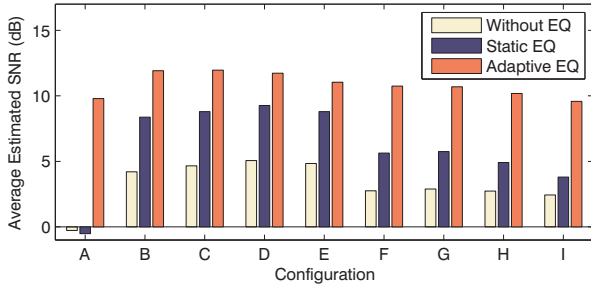


Fig. 5. Average single receiver element estimated SNR for all configurations, prior to equalization and also after both equalization techniques. Table II lists Doppler estimation configurations.

IV. EXPERIMENTAL RESULTS

The average SNR estimates from the individual Doppler compensation techniques, as well as the average SNR estimates after equalization are shown in Fig. 5. The packet-wide frequency offset detection (Config. A) offered by self-referenced correlation performs the worst of all Doppler compensation configurations (before equalization). Since Config. A estimates frequency offset from a series of symbols that comprise $\sim 1.2\%$ of the entire packet data sequence, only the corresponding Doppler effects observed in that subset of time are represented in the estimate. On the other hand, the DFT technique with three windows (Config. D) performs the best, closely followed by other DFT window configurations.

Details on equalizer performance can be found in Fig. 6. Column headings denote the use of static and adaptive equalizers, while the main portion shows the results of each individual decoding operation corresponding with one sampled packet (grouped among individual receivers within the 5-receiver array). These groupings are then arranged sequentially according to received packet, as 5 or 6 packets were transmitted at each position. Lighter shades signify successful decoding operations; darker shades signify failure.

An important characteristic of the BER visualizations is evidence of catastrophic failures. A BER of around 0.5 often coincides with a failure of frame synchronization or Doppler correction. Such failure exceeds the capabilities of equalizers to correct the problem. It is also possible for the adaptive equalizer to respond in undesirable ways to noise or other channel effects, although we had found that under most circumstances this was not the case. For reference, the percentage of packets that yielded a BER of more than 0.05—an upper threshold for a possible error correction code configuration—is shown in Fig. 7.

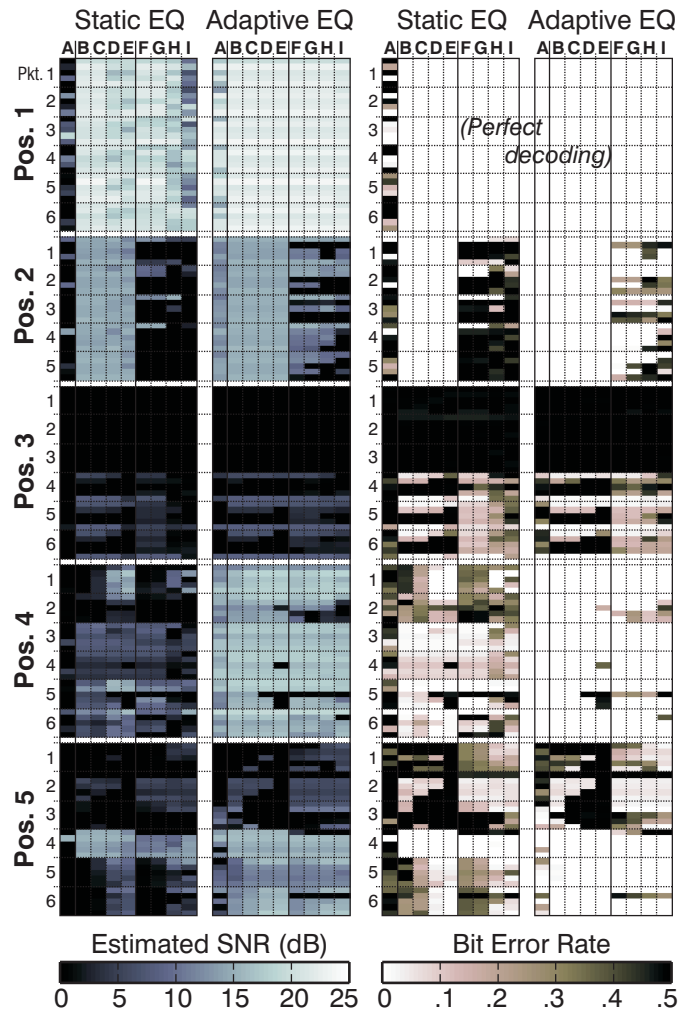


Fig. 6. SNR and BER performance of QPSK single element receiver at five positions given in Table I using the configurations listed in Table II.

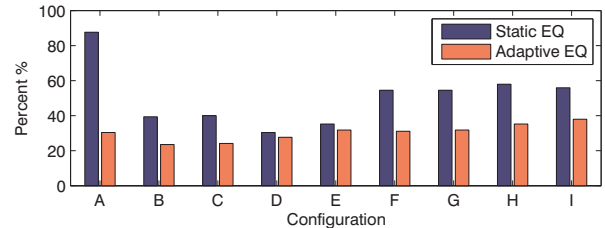


Fig. 7. Percentage of packets (of the 145 analyzed) with BER > 0.05

One intriguing observation that was evident in some packets was the corruption of pilot tone phase (Configs. F-I in Fig. 6). Fig. 8 shows inconsistencies among pilot tones that were tracked among the 5 receivers simultaneously using a PLL-type algorithm. Although further analysis is needed, it is highly likely that multiple paths are causing selective fading at the receivers, making the algorithm lose accuracy.

We had observed that the accuracy of Doppler detection using the DFT and pilot tone analysis techniques can be diminished when windows grow small (see Fig. 9). One logical

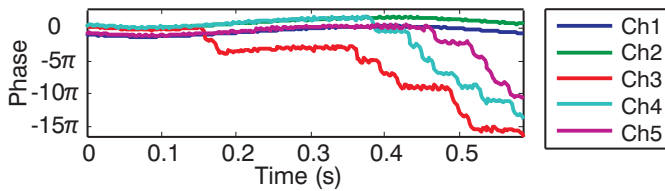


Fig. 8. Comparison of bulk frequency offset corrected pilot tone phase (unwrapped) among 5 simultaneous channels at Pos. 5. Note that ideal operation would result in consistency among the channels.

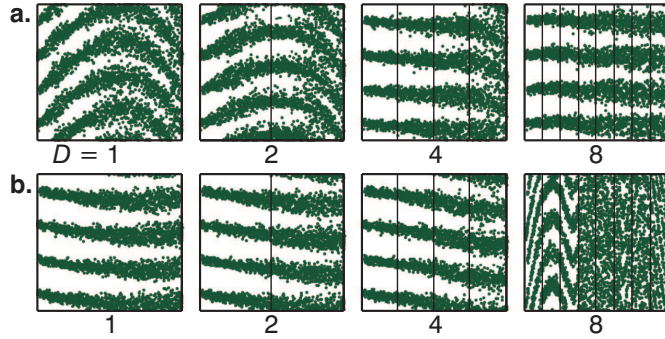


Fig. 9. The effects of window size on phase of a received QPSK signal over 250ms. In (a), increasing window count D improves Doppler compensation, decreasing bit error rate. In (b), increased window count D results in poor estimates, increasing bit error rate. See Fig. 2 for axis labels.

cause is the presence of phase noise; larger windows involve the averaging of more samples, thus reducing the effects of noise. For the DFT technique, our use of the FFT operation requires zero-padding of the data sequence in order to facilitate frequency bins that are small enough to offer our desired frequency resolution. This comparative reduction in data (as well as the greater influence of noise) diminishes the ability to measure a distinct dominant frequency.

One feature of these results is that the use of finer windowing has potential of yielding a vastly improved signal to noise ratio when using the static equalizer in the motion tests (Pos. 4 and 5). But, it is also evident that finer windowing imposes more risk, increasing the likelihood of catastrophic failure, as seen in Pos. 2. Given ample computing capabilities, it is conceivable that optimal performance in a deployed communications system can be realized through implementation of parallel approaches. Decision logic can then determine whether the riskier approach has undergone catastrophic failure and can select the more reliable approach.

This analysis revealed three important observations. First, there was merit in using the improved Doppler estimation technique in conjunction with a static equalizer. Gains of up to 10-15dB SNR were realized in certain examples. Second, our pilot tone frequency measurement method did not appear to be a reliable way to detect Doppler effects. We believe that this was due to selective fading as caused by multipath interference at the receiver. Third, the most reliable configuration over the entire data set was the single window DFT estimate with the adaptive equalizer.

V. CONCLUSION

This project demonstrated a successful implementation of a communication system for the shallow underwater acoustic channel and a framework to evaluate improved Doppler estimation techniques. In our joint Doppler tracking/equalization tests, the use of a single window bulk DFT estimate and adaptive DFE gave the most reliable results.

The 360 packets of data from the 5 receiver array elements is available for download at <http://users.ece.utexas.edu/~bevans/projects/underwater/datasets/>.

ACKNOWLEDGMENT

This research was supported by Independent Research and Development funds from the Applied Research Laboratories at The University of Texas at Austin in Austin, Texas.

REFERENCES

- [1] J. Preisig, "Acoustic propagation considerations for underwater acoustic communications network development," *SIGMOBILE Mobile Computing and Communications Review*, vol. 11, pp. 2–10, Oct. 2007.
- [2] T. Kang and R. Iltis, "Fast-varying doppler compensation for underwater acoustic OFDM systems," in *Proc. IEEE Asilomar Conf. on Signals, Systems and Computers*, Oct. 2008, pp. 933–937.
- [3] D. Kilfoyle and A. Baggeroer, "The state of the art in underwater acoustic telemetry," *IEEE Journal of Oceanic Engineering*, vol. 25, no. 1, pp. 4–27, Jan. 2000.
- [4] M. Chitre, S. Shahabudeen, L. Freitag, and M. Stojanovic, "Recent advances in underwater acoustic communications and networking," in *Proc. IEEE Oceans 2008*, Sept. 2008, pp. 1–10.
- [5] M. Stojanovic, "Recent advances in high-speed underwater acoustic communications," *IEEE Journal of Oceanic Engineering*, vol. 21, no. 2, pp. 125–136, Apr. 1996.
- [6] R. Urick, *Principles of Underwater Sound*, 3rd ed. Peninsula, 1996.
- [7] K. Nieman, K. Perrine, K. Lent, T. Henderson, T. Brudner, and B. Evans, "Multi-stage and sparse equalizer design for communication systems in reverberant underwater channels," in *Proc. IEEE Workshop on Signal Processing Systems Design and Implementation*, Oct. 2010.
- [8] M. Stojanovic, J. Catipovic, and J. Proakis, "Phase-coherent digital communications for underwater acoustic channels," *IEEE Journal of Oceanic Engineering*, vol. 19, no. 1, pp. 100–111, Jan 1994.
- [9] M. R. Ducoff and B. W. Tietjen, *Radar Handbook*, 3rd ed. McGraw-Hill, 2008, ch. Pulse Compression Radar, pp. 8.3–8.11.
- [10] P. Moose, "A technique for orthogonal frequency division multiplexing frequency offset correction," *IEEE Transactions on Communications*, vol. 42, no. 10, pp. 2908–2914, Oct. 1994.
- [11] C. R. Johnson and W. A. Sethares, *Telecommunication Breakdown*. Prentice Hall, 2004.
- [12] V. Torres, A. Perez-Pscual, T. Sansaloni, and J. Valls, "Design of high performance timing recovery loops for communication applications," in *IEEE Workshop on Signal Processing Systems Design and Implementation*, Oct. 2006, pp. 1–4.
- [13] M. Johnson, L. Freitag, and M. Stojanovic, "Improved Doppler tracking and correction for underwater acoustic communications," in *IEEE International Conference on Acoustics, Speech, and Signal Processing*, vol. 1, Apr 1997, pp. 575–578 vol.1.
- [14] B. Li, S. Zhou, M. Stojanovic, L. Freitag, and P. Willett, "Non-uniform Doppler compensation for zero-padded OFDM over fast-varying underwater acoustic channels," in *Proc. IEEE Oceans Europe, June 2007*, pp. 1–6.
- [15] D. Lucani, M. Medard, and M. Stojanovic, "Capacity scaling laws for underwater networks," in *Proc. Asilomar Conference on Signals, Systems and Computers*, Oct. 2008, pp. 2125–2129.
- [16] Lower Colorado River Authority, "Historical lake levels: Highland lakes," <http://www.lcra.org/water/conditions/historical.html>, 2007.
- [17] J. G. Proakis, *Digital Communications*, 2nd ed. McGraw-Hill, 1989, pp. 638–642, 660–668.
- [18] T. Oberg, B. Nilsson, N. Olofsson, M. Nordenvaad, and E. Sangfelt, "Underwater communication link with iterative equalization," in *Proc. IEEE Oceans*, Sept. 2006, pp. 1–6.